Vol 446|5 April 2007|doi:10.1038/nature05718

LETTERS

Global warming and climate forcing by recent albedo changes on Mars

Lori K. Fenton[1], Paul E. Geissler[3] & Robert M. Haberle[2]

For hundreds of years, scientists have tracked the changing appearance of Mars, first by hand drawings and later by photographs[1,2]. Because of this historical record, many classical albedo patterns have long been known to shift in appearance over time. Decadal variations of the martian surface albedo are generally attributed to removal and deposition of small amounts of relatively bright dust on the surface. Large swaths of the surface (up to 56 million km^2) have been observed to darken or brighten by 10 per cent or more[3–5]. It is unknown, however, how these albedo changes affect wind circulation, dust transport and the feedback between these processes and the martian climate. Here we present predictions from a Mars general circulation model, indicating that the observed interannual albedo alterations strongly influence the martian environment. Results indicate enhanced wind stress in recently darkened areas and decreased wind stress in brightened areas, producing a positive feedback system in which the albedo changes strengthen the winds that generate the changes. The simulations also predict a net annual global warming of surface air temperatures by ~0.65 K, enhancing dust lifting by increasing the likelihood of dust devil generation. The increase in global dust lifting by both wind stress and dust devils may affect the mechanisms that trigger large dust storm initiation, a poorly understood phenomenon, unique to Mars. In addition, predicted increases in summertime air temperatures at high southern latitudes would contribute to the rapid and steady scarp retreat that has been observed in the south polar residual ice for the past four Mars years[6–8]. Our results suggest that documented albedo changes affect recent climate change and large-scale weather patterns on Mars, and thus albedo variations are a necessary component of future atmospheric and climate studies.

Thermal Emission Spectrometer (TES) broadband albedos from the years 1999–2000 are shown in Fig. 1a, which has been artificially tinted a rust colour that mimics the apparent visible colour of Mars. In Fig. 1b, changes in albedo since the Viking mission are highlighted. Many areas on Mars darkened at some time during the 20-year interval between the Viking and Mars Global Surveyor (MGS) missions, particularly those regions associated with high thermal inertia[4]. Northern dark areas, such as Acidalia Planitia and northern Utopia

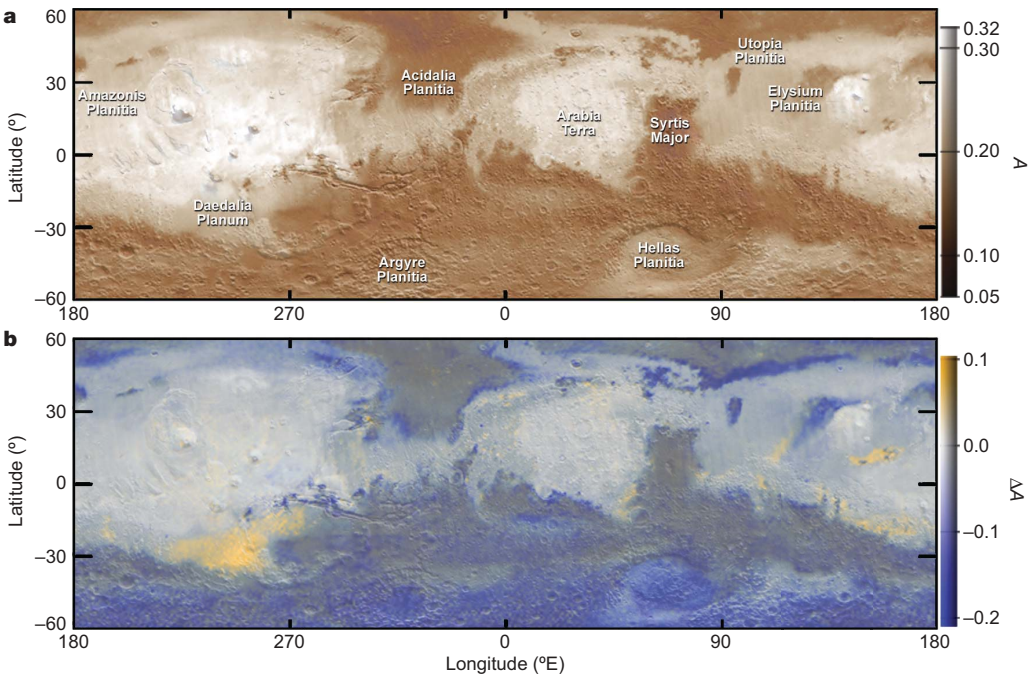

Figure 1 | Albedo and changes in albedo. a, Albedo map of Mars superimposed on Mars Orbiter Laser Altimeter (MOLA) shaded relief. Albedos (A) are calculated from the broadband TES bolometer: the rust tint is artificially applied to approximate the appearance of the martian surface. **b**, TES albedos in greyscale superimposed on MOLA shaded relief, with changes (ΔA) relative to the Viking IRTM shown in yellow for relative brightening and blue for relative darkening (see scale on right).

[1]Carl Sagan Center, [2]Space Science Division, NASA Ames Research Center, Moffett Field, California 94035, USA. [3]US Geological Survey, Flagstaff, Arizona 86001, USA.

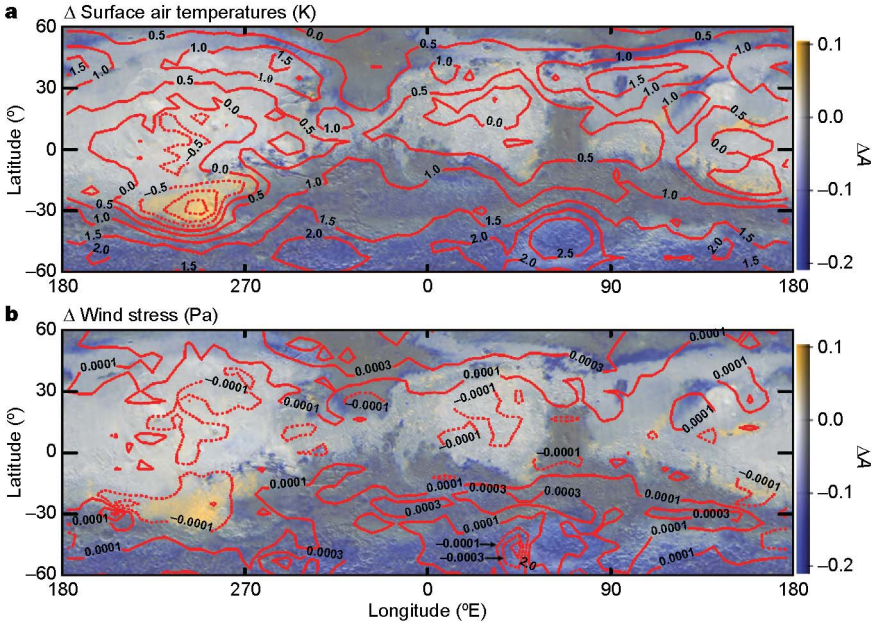

Figure 2 | The effect of albedo changes on air temperature and wind stress. **a**, MGCM-predicted annual-mean change in surface air temperatures (TES−IRTM; contours) on the same plot from Fig. 1. Note the temperature increases over darkened surfaces and temperature decreases over brightened surfaces. **b**, MGCM-predicted annual-mean change in wind stress (TES−IRTM; contours). Note the general correlation of wind stress increases over darkened surfaces and wind stress decreases over brightened surfaces.

Planitia, expanded southwards. Nearly the entire southern mid-latitude zone between −40° and −70° darkened, including Argyre and Hellas Planitiae. This darkening of the Southern Highlands is especially important because of the enhanced insolation during southern summer, when Mars is closest to the Sun. Most of the areas that brightened are located on the southern edges of high-albedo regions, such as Daedalia Planum. The only large regions that remained unchanged are the bright, dust mantled, low thermal inertia 'continents', such as Amazonis Planitia and Arabia Terra.

Earlier comparisons of atmospheric temperatures derived from MGS and Viking data indicated that most differences were caused by the temporally and spatially varying patterns of suspended atmospheric dust[9]. As the MGS mapping mission continued, further studies revealed differences not caused by atmospheric dust loading: for example, night-time atmospheric temperatures are repeatable from one Mars year to the next, but daytime atmospheric temperatures are more variable[10,11]. In particular, measurements from TES following the 2001 global dust storm (GDS) indicate that 4 K cooler daytime atmospheric temperatures persisted throughout the aphelion season following the storm, despite the facts that atmospheric dust opacities had long since dropped to pre-storm values and that night-time temperatures appeared consistent with previous years. This post-storm daytime cooling was attributed to deposition of bright dust on the surface after the dust storm, causing the albedo to increase, and subsequently reducing both surface and atmospheric temperatures[11]. Thus, interannual variations in dust fallout on the martian surface have had a measurable effect on atmospheric temperatures.

We applied two maps of surface Lambert albedo to the NASA Ames Mars general circulation model (MGCM)[12]; we used version 1.7.3 of the MGCM with an Arakawa C-grid (in which zonal and meridional winds are staggered horizontally between the main longitudinal and latitudinal grid point positions, respectively). One map was produced from the Infrared Thermal Mapper (IRTM) on the Viking Orbiters, derived from calibrated data obtained during non-dusty periods of the first and second years of the Viking mission (1976–78)[3,13,14]. The second map was produced from TES albedos derived from calibrated data obtained during non-dusty periods during the first year of the MGS mapping mission (1999–2000)[15]. The two measurements span very similar wavelength ranges (0.3–3.0 μm for IRTM[16] and 0.3–2.9 μm for TES[15]), and thus are directly comparable. Because the original IRTM albedo map spans latitudes between ±60°, TES albedos were substituted in areas poleward of this boundary. Thus, there is no effective change in albedo in the polar regions and higher latitudes in these model runs. In each case, the MGCM was run for a full model year (following a spin-up year), with a horizontal grid spacing of 6° of longitude by 5° of latitude, and 24 vertical atmospheric levels ranging from the surface to a pressure of 0.0005 mbar (~100 km). The visible dust opacity was set to a constant value of 0.3 on a 6.1-mbar pressure surface. Although a simplification of the martian dust cycle, this dust scheme ensures that differences in wind circulation and other parameters are caused solely by surface forcing from albedo changes.

Differencing of atmospheric parameters from the MGCM output demonstrates that the albedo fluctuations do drive some atmospheric changes. Table 1 lists annual global-mean changes of several parameters, calculated by averaging the difference of each parameter in each grid point and time step, weighted by the zonal-mean spatial area in each grid point. Although the changes are slight, annual

Table 1 | Annual global-mean values predicted by the MGCM

Parameter	IRTM	TES	$\Delta_{TES-IRTM}$	$\%\Delta_{TES-IRTM}$
Ground temperature	201.58 K	202.43 K	+0.86 K	+0.42%
Surface air temperature	195.61 K	196.26 K	+0.65 K	+0.33%
Condensed CO_2	5.83×10^{12} kg	5.79×10^{12} kg	-3.62×10^{10} kg	−0.62%
Daytime planetary boundary layer	0.85 km	0.88 km	+0.02 km	+2.7%
Wind stress	3.49×10^{-3} Pa	3.56×10^{-3} Pa	$+0.07 \times 10^{-3}$ Pa	+2.9%
Surface wind speed	6.76 m s^{-1}	6.84 m s^{-1}	+0.08 m s^{-1}	+1.3%

global-mean values are not representative of more dramatic changes on smaller spatial and temporal scales. Furthermore, small but steady changes acting on a timescale of decades could lead to much larger cumulative shifts in climate-influencing processes. Ground and surface air temperatures increase slightly as a result of the global-mean decrease in albedo and subsequent increase in absorbed solar energy on the surface. In particular, the surface air temperature increase of ~0.65 K is a value on the same scale as that of measured interannual variations of land-surface air temperatures on Earth, even though the processes involved are significantly different[17]. Increased heating near the surface leads to greater convective instability, pushing the planetary boundary layer slightly higher. Surface wind stresses increase slightly, largely as a result of increases in the magnitude of near-surface wind velocity. Because the observed global annual-mean differences in Table 1 are small, sensitivity tests of the MGCM are useful in determining the reliability of these numbers. Adding an initial perturbation or running at a different resolution produced changes that were at least an order of magnitude smaller than those produced by albedo changes, and so the model results presented here are considered robust.

Figure 2 shows the albedo-driven differences in annual-mean surface atmospheric temperatures and wind stresses as a function of latitude and longitude. Warmer temperatures and higher wind stresses correlate with the areas where the albedo decreased, and cooler temperatures and lower wind stresses generally correlate with areas that brightened. Previous work has shown that martian albedo changes within the range discussed in this work can locally change the predicted planetary boundary layer depth by more than a kilometre, which could significantly influence dust devil generation[18]. One model of dust devil formation treats these vortices as heat engines, with a thermodynamic efficiency related to the depth of the planetary boundary layer[19]. Thus a decrease in surface albedo could contribute to enhanced dust lifting for two reasons: (1) increased wind stresses directly lift more particulate material (both dust and sand) off the surface, and (2) a more unstable atmosphere will lead to a higher dust devil generation rate, lifting more dust into the atmosphere. The coupling of these processes with albedo changes could produce a positive feedback mechanism of surface–atmosphere interaction, in which surface albedo reductions enhance the dust lifting processes that produce the surface changes.

Moreover, a change in global surface albedo could influence the formation of dust storms, both on local and global scales. It has been suggested that the surface brightening and atmospheric cooling following the 2001 GDS may affect the timing of future large dust storms[11]. Indeed, our work shows that a surface brightening caused by dust fallout would decrease wind stresses and suppress dust devil formation, the two mechanisms potentially responsible for dust storm initiation. Our results indicate that widespread dust fallout from one GDS-bearing year would make it more difficult for a GDS to occur in the following years. The lack of continuity in the historical record of GDS occurrence makes it difficult to test this hypothesis, but the exceptions of large storms in four successive Mars years from 1971–77[20,21] indicate that other factors must also be in play and able to overcome (on occasion in a single year) the significant effects of albedo changes due to dust deposition. The relatively high number of dust storms of the 1970s appears to have contributed to higher Viking albedos relative to those measured by MGS in 1999–2000, which followed a decade or more of relative inactivity[5]. If global surface albedo affects dust storm initiation (and is itself affected by dust storm fallout), then long term trends in albedo change could dictate decadal periods prone to large dust storms versus periods free of such storms. Although the events that trigger dust storms (in particular, GDSs) have yet to be fully understood, this work demonstrates that one contributing factor may be a decrease in surface albedo. Thus, a realistically time-varying surface albedo must be included in future atmospheric simulations in order to accurately represent the dust cycle.

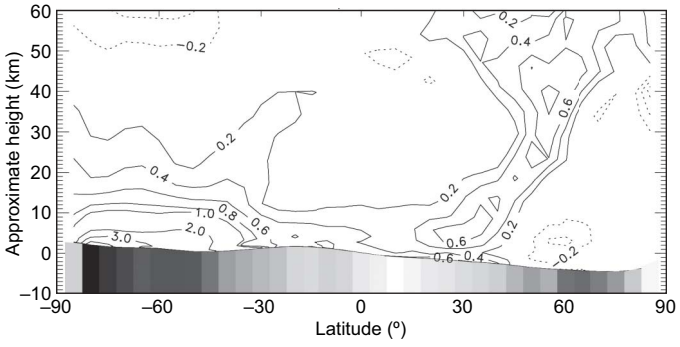

Figure 3 | MGCM air temperature differences during perihelion season. Zonal-mean air temperature differences (TES−IRTM) as a function of approximate elevation and latitude for $L_s = 260°$–$280°$. Raw temperatures were interpolated onto constant pressure surfaces before averaging. Zonal-mean surface level is plotted at the bottom, with zonal-mean differences in albedo changes shown in greyscale beneath the surface (white, $\Delta A = +0.001$; black, $\Delta A = -0.088$; MOLA elevation datum refers to ~6.1-mbar pressure level). Note that contours smaller than 1 K are shown in 0.2 K intervals; contours greater than 1 K are shown in 1 K intervals. Air temperatures above the south polar residual cap increase by 3–4 K near the surface, probably enhancing scarp retreat in the residual polar ice cap.

Erosion of depression walls in the southern residual polar cap has been observed by the Mars Orbiter Camera (MOC) during the MGS mission, suggesting that short-term climate change is currently occurring on Mars[6]. Further study has led to the proposal that over the last 100–150 martian years the southern residual polar cap has undergone a series of short depositional periods followed by longer periods (on the order of one or more decades) of erosion by scarp retreat[8]. According to this analysis, the most recent CO_2 ice layer may have been deposited shortly after 1972. It is postulated that these periods of deposition and erosion may be linked to dust storm frequency or changes in surface albedo[8]. If dust storms were responsible, then the youngest residual ice layer would have been deposited as a result of atmospheric changes caused by the 1971 GDS. However, the relationship between GDSs and polar cap erosion is problematic, because multiple year coverage from MOC indicates that no permanent ice layer was deposited in the aphelion season (southern winter) after the 2001 GDS[6], despite the storm-related atmospheric cooling and surface brightening[10,11]. It is also likely that no additions were made to the residual ice cap in winters following the 1973–77 GDSs. It appears that the southern residual ice cap was in a state of erosion during the period between the late 1970s up to the present.

To investigate albedo-driven changes at high latitudes, we reran the IRTM albedo case, this time including IRTM albedos spanning latitudes ±80°. IRTM albedos poleward of ±60° were derived using an atmospherically corrected subsurface conduction model[22–24]. Recently reported emission angle effects may cause the actual high-latitude TES–IRTM albedo differences to be smaller than those applied here[5], potentially lessening the following results. Figure 3 shows that zonal-mean summertime temperatures over the southern polar cap increased by 0.2–2 K poleward of −85° from the surface up to an altitude of ~30 km. The subsequent increase in emitted downwelling infrared radiation predicted by the MGCM in grid points spanning the residual polar cap is ~1 W m^{-2}. If this entire increase in infrared radiation goes into sublimating residual CO_2 ice, the potential mass loss during the southern summer (when the solar longitude $L_s = 250°$–$350°$) is $\sim 5 \times 10^{12}$ kg. Previous estimates of summertime CO_2 mass loss from the south polar residual cap, based on observations of scarp retreat, range from 8.4×10^{12} kg (ref. 8) to $(2–4) \times 10^{13}$ kg (ref. 6). Assuming that all other polar processes (for example, cloud condensation, spatially varying atmospheric dust) cancel out between the IRTM and TES model runs, surface darkening at high southern latitudes could contribute substantially

to permanent erosion of CO_2 deposits, probably preventing recondensation in any potential cold traps.

Martian climate indicators, such as GDS occurrence, polar energy balance, and annual global-mean air temperature, are dependent on many interrelated and poorly understood processes. By investigating solely the effects of changes in surface albedo (from two very different Mars years), we have shown that albedo interacts with, and could in part drive, other climate-influencing processes on Mars.

Received 6 September 2006; accepted 22 February 2007.

1. Flammarion, C. *La Planète Mars et ses Conditions d'Habitabilité* Vols 1 and 2 (Gauthier Villars et Fils, Paris, 1892).
2. de Vaucouleurs, G. *Physics of the Planet Mars* (Faber and Faber, London, 1954).
3. Christensen, P. R. Global albedo variations on Mars: Implications for active aeolian transport, deposition, and erosion. *J. Geophys. Res.* **93** (B7), 7611–7624 (1988).
4. Geissler, P. E. Three decades of Martian surface changes. *J. Geophys. Res.* **110,** E02001, doi:10.1029/2004JE002345 (2005).
5. Szwast, M. A., Richardson, M. I. & Vasavada, A. R. Surface dust redistribution on Mars as observed by the Mars Global Surveyor and Viking Orbiters. *J. Geophys. Res.* **111,** E11008, doi:10.1029/2005JE002485 (2006).
6. Malin, M. C., Caplinger, M. A. & Davis, S. D. Observational evidence for an active surface reservoir of solid carbon dioxide on Mars. *Science* **294,** 2146–2148 (2001).
7. Byrne, S. & Ingersoll, A. P. A sublimation model for Martian south polar ice features. *Science* **299,** 1051–1053 (2003).
8. Thomas, P. C. *et al.* South polar residual cap of Mars: Features, stratigraphy, and changes. *Icarus* **174,** 535–559 (2005).
9. Clancy, R. T. *et al.* An intercomparison of ground-based millimetre, MGS TES, and Viking atmospheric temperature measurements: Seasonal and interannual variability of temperatures and dust loading in the global Mars atmosphere. *J. Geophys. Res.* **105** (E4), 9553–9571 (2000).
10. Liu, J., Richardson, M. I. & Wilson, R. J. An assessment of the global, seasonal, and interannual spacecraft record of Martian climate in the thermal infrared. *J. Geophys. Res.* **108** (E8), 5089, doi:10.1029/2002JE001921 (2003).
11. Smith, M. D. Interannual variability in TES atmospheric observations of Mars during 1999–2003. *Icarus* **167,** 148–165 (2004).
12. Haberle, R. M. *et al.* General circulation model simulations of the Mars Pathfinder atmospheric structure investigation/meteorology data. *J. Geophys. Res.* **104** (E4), 8957–8974 (1999).
13. Kieffer, H. H. *et al.* Thermal and albedo mapping of Mars during the Viking primary mission. *J. Geophys. Res.* **82,** 4249–4292 (1977).
14. Pleskot, L. K. & Miner, E. D. Time variability of martian bolometric albedo. *Icarus* **45,** 179–201 (1981).
15. Christensen, P. R. *et al.* Mars Global Surveyor Thermal Emission Spectrometer experiment: Investigation description and surface science results. *J. Geophys. Res.* **106** (E10), 23823–23872 (2001).
16. Kieffer, H. H., Davis, P. A. & Soderblom, L. A. Mars' global properties — Maps and applications. *Proc. Lunar Planet. Sci. Conf.* **XII,** 1395–1417 (1982).
17. Houghton, J. T., *et al. Climate Change: The Scientific Basis* 105–107 (Cambridge Univ. Press, New York, 2001).
18. Kahre, M. A. *et al.* Observing the martian surface albedo pattern: Comparing the AEOS and TES data sets. *Icarus* **179,** 55–62 (2005).
19. Rennó, N. O., Burkett, M. L. & Larkin, M. P. A simple thermodynamical theory for dust devils. *J. Atmos. Sci.* **55,** 3244–3252 (1998).
20. Zurek, R. W. & Martin, L. J. Interannual variability of planet-encircling dust storms on Mars. *J. Geophys. Res.* **98** (E2), 3247–3259 (1993).
21. McKim, R. Telescopic Martian dust storms: A narrative and catalogue. *Mem. Br. Astron. Assoc.* **44,** 1–168 (1999).
22. Vasavada, A. R. *et al.* Surface properties of Mars' polar layered deposits and polar landing sites. *J. Geophys. Res.* **105** (E3), 6961–6970 (1999).
23. Paige, D. A., Bachman, J. E. & Keegan, K. D. Thermal and albedo mapping of the polar regions of Mars using Viking thermal mapper observations, 1, North polar region. *J. Geophys. Res.* **99** (E12), 25959–25992 (1994).
24. Paige, D. A. & Keegan, K. D. Thermal and albedo mapping of the polar regions of Mars using Viking thermal mapper observations, 2, South polar region. *J. Geophys. Res.* **99** (E12), 25993–26014 (1994).

Acknowledgements We thank J. Schaeffer for help with the MGCM, and T. Michaels and R. Zurek for comments and suggestions. This work was supported by the NASA Mars Data Analysis Program.

Author Information Reprints and permissions information is available at www.nature.com/reprints. The authors declare no competing financial interests. Correspondence and requests for materials should be addressed to L.K.F. (fenton@mintz.arc.nasa.gov) or P.E.G. (pgeissler@usgs.gov).